Biophysical Chemistry, 38 (1990) 189–199
Elsevier

BIOCHE 01441

A model equation for the gravielectric effect in electrochemical cells

A. Ślęzak

Department of Biophysics, Silesian Medical Academy, Karol Marx Str. 19, 41-808 Zabrze 8, Poland

Received 16 July 1989
Revised manuscript received 24 December 1989
Accepted 24 December 1989

Gravielectric effect; Membrane transport; Rayleigh-Taylor convective instability

The gravielectric effect model equation for a single-membrane system was elaborated. This model for binary and ternary ionic solutions was verified using a cell with a horizontally mounted membrane. In this cell, the membrane and transition potentials were measured as a function of gravitational configuration. In these experiments, a 0.001 M aqueous solution of sodium chloride was placed on one side of the membrane. The opposite side of the membrane was exposed to either aqueous sodium chloride solutions, with densities greater than that of 0.001 M aqueous NaCl, or ethanol/NaCl/water solutions. On the basis of the experimental results, the influence of constrained release and the gravielectric effect were established. These experimental findings are interpreted in terms of a convective gravitational instability that reduces boundary layer dimensions and increases the permeability coefficient of the complex system: boundary layer/membrane/boundary layer. A concentration-gradient Rayleigh number is used in a mathematical model for gravitationally sensitive membrane potential.

1. Introduction

The gravitational field exerts a relatively strong influence on living organisms and is one of the main evolutionary factors in the development and modification of modern forms of life on Earth [1]. This field regulates bioenergetic processes to a great extent and also determines the size, proportions and shape of biological objects [2].

Under terrestrial conditions, living organisms (plants and animals) remain in a relatively stable gravitational field. The need for constant spatial orientation in relation to the field has resulted in the formation of more or less complicated gravireceptors and supporting structures in most terrestial organisms during the course of evolutionary processes [3–6]. The influence of the gravitational field on plants manifests itself in phenomena such as gravitropism, the gravielectric effect and gravimorphism [5–15]. In microorganisms gravitaxis has been observed [6].

The first observation of the gravielectric effect (GEE) was made by Bose [8] in 1907 in petioles of *Trophaedum* for which the author discovered that the change in orientation of this organ from a vertical to a horizontal position generated a potential difference across it, its underside being positively charged with respect to the upper part. In 1926, Brauner [9] observed an electrical polarization effect in an electrochemical cell similar to that described by Bose in plants. On this basis, he designated both phenomena as the geoelectric effect (now called the gravielectric effect). Studies on the GEE performed during the subsequent years led to the description of this phenomenon in organs and in single cells [10–15].

Investigations of the GEE carried out by Brauner [9–11], and by Custard and Faris [16] in

Correspondence address: A. Ślęzak, Department of Biophysics, Silesian Medical Academy, Karol Marx Str. 19, 41-808 Zabrze 8, Poland.

electrochemical systems were resolved by measurement of the temporal change in potential at two extreme (horizontal and vertical) positions of the membrane. Those authors accordingly believe that the gravitational field is the factor responsible for the occurrence of the GEE in electrochemical systems. Moreover, Brauner claimed that the gravitational field influenced the kinetics of vertical ion transport, leading to the separation of both anions and cations and to the generation of, or change in, a membrane potential.

Custard and Faris claimed that the gravitational field was the underlying cause for the appearance of a stable layer of the solution, above the upper surface of a horizontally mounted membrane, which diminishes the transfer number of ions present in interfacial regions which leads to a change (decrease or increase) in the value of the membrane potential. In their opinion, the tangential action of the gravitational field, when the membrane is oriented in a vertical position, destroys the layer and causes an increase in transfer number, thereby leading to an increase in membrane potential. The reverse process leads to a fall in the transport number and a subsequent decrease in membrane potential. It is difficult to accept their interpretations as being valid because of the following aspects:

(a) The gravitational field is very weak and the assumption that it could manifest itself against the background of a strong electrostatic field is not justifiable;

(b) It has been shown [17–26] that there is a common tendency to form boundary layers on both sides of the membrane, thus reducing osmotic and diffusive transmembrane transport.

Studies concerning gravitational effects in osmotic and diffusive transport of non-electrolytes across a horizontally mounted membrane [22–26] constitute definite progress in the recognition of the mechanism of GEE generation in a single-membrane system. In the papers cited, it has been shown that the boundary layers formed on both sides of a membrane have different degrees of hydrodynamical stability [25,26] which depends on the position of the membrane in relation to the gravitational vector. If the membrane is oriented in a horizontal plane and the density gradient in the solutions separated by the membrane is parallel to this vector, then Rayleigh-Taylor instability may appear in the system [25,26]. Instability of this type has been observed in systems with a vertically mounted membrane [24]. Rayleigh-Taylor instability in systems with a horizontally mounted membrane does not occur when the density gradient is antiparallel to the gravitational vector. Stability of the boundary layers results in a substantial reduction in transmembrane flux; instability of the boundary layers minimizes its thickness and the extent of flux reduction.

A membrane system containing electrolyte solutions has analogous hydrodynamical properties. These properties as manifested in the membrane potential are described in the current paper. In addition, a physical interpretation of the gravielectric effect is given, based on the formalism proposed by Rejou-Michel et al. [21] and Rayleigh-Taylor analysis of fluid gravitational stability.

2. Determination of the physical nature of gravielectric effect

Let us consider a membrane system such as that presented in fig. 1. We assume that the membrane system consists of n membranes separating aqueous solutions of one electrolyte. Moreover, we assume that the n-membrane system consists of a number of single-membrane systems, which will be considered independently using the formalism of Rejou-Michel et al. [21]. Let the solutions fulfill the condition

$$C_1 < C_2 < \cdots < C_{n-1} < C_n. \tag{1}$$

Consider three gravitational configurations (A, B_1 and B_2) of this n-membrane system. In configura-

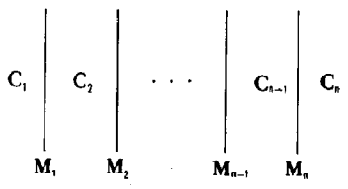

Fig. 1. The n-membrane system.

tion A, the membranes are oriented in vertical planes and in B_1 and B_2 in horizontal planes, the respective concentration gradients for the latter two configurations being antiparallel and parallel to the gravitational vector.

According to the formalism of Rejou-Michel et al. [21] for the effect of constraints release (ECR) in an n-membrane system, we can write

$$(\overline{\mathrm{ECR}})_j = \sum_{i=1}^{n} (\mathrm{ECR})_{ij}, \qquad j = 0, 1, 2, \tag{2}$$

and

$$(\mathrm{ECR})_i = \sum_{i=1}^{n} (\psi_\mathrm{T} - \psi_\mathrm{M})_i, \tag{3}$$

where indices 0, 1, 2 pertain to configurations A, B_1 and B_2, respectively, ψ_T denotes the transition potential, ψ_M the membrane potential and $(\mathrm{ECR})_i$ the effect of constraints release for the i-th membrane.

Combining eqs 2 and 3, we obtain

$$(\overline{\mathrm{ECR}})_j = \sum_{i=1}^{n} (\psi_\mathrm{T} - \psi_\mathrm{M})_{ij}. \tag{4}$$

In turn, using the expression

$$\psi_\mathrm{M} = \sum_{i=1}^{n} (\psi_\mathrm{L} + \psi_\mathrm{S})_i, \tag{5}$$

eq. 4 can be expressed as

$$(\overline{\mathrm{ECR}})_j = \sum_{i=1}^{n} (\psi_\mathrm{T} - \psi_\mathrm{L})_{ij} - \sum_{i=1}^{n} (\psi_\mathrm{S})_{ij}, \tag{6}$$

where ψ_L is the liquid junction potential and ψ_S the specific contribution.

If we assume [21] that $(\psi_\mathrm{T} - \psi_\mathrm{L})_{ij} = 0$, we obtain

$$(\overline{\mathrm{ECR}})_j = -\sum_{i=1}^{n} (\psi_\mathrm{S})_{ij}. \tag{7}$$

In this way we have defined the effect of the constraints release for a three gravitational configuration of the n-membrane system. The definition of the GEE can now be formulated as follows:

$$(\mathrm{GEE})_k = (\overline{\mathrm{ECR}})_k - (\overline{\mathrm{ECR}})_0, \qquad k = 1, 2. \tag{8}$$

Combining eqs 4 and 8, we obtain

$$(\mathrm{GEE})_k = \sum_{i=1}^{n} [(\psi_{\mathrm{T}k} - \psi_{\mathrm{T}0})_i + (\psi_{\mathrm{M}0} - \psi_{\mathrm{M}k})_i]. \tag{9}$$

In turn, using eq. 7, eq. 8 can be expressed as:

$$(\mathrm{GEE})_k = \sum_{i=1}^{n} (\psi_{\mathrm{S}0} - \psi_{\mathrm{S}k})_i. \tag{10}$$

We have formulated two definitions of the GEE. The second, represented by eq. 10, allows for theoretical analysis of the GEE. In the subsequent section, the physical sense of the specific contribution (ψ_S) is described.

3. Phenomenological description of the specific contribution (ψ_S)

Definition of the potential ψ_S is possible only in relation to the membrane potential (ψ_M). Hence, the analysis is begun be presenting the equation for the diffusive membrane potential, based on the method of Rejou-Michel et al. [21]. The equation can be expressed as:

$$\psi_\mathrm{M} = -\frac{RT}{F} \sum_{r=1}^{m} \int_l^h t_r \, \mathrm{d} \ln C_r, \tag{11}$$

where RT is the product of the gas constant and absolute temperature, F the Faraday constant, t_r the transfer number, l and h the lower and higher concentrations of the membrane and solution component and C_r the concentration of the r-th component of the membrane.

If the inhomogeneity of the density (concentration) connected with the formation of diffusion boundary layers on both sides of the membrane appears in regions of the solution which are close to the membrane, the right-hand side of eq. 11 is then expressed as:

$$\psi_\mathrm{M} = -\frac{RT}{F} \sum_{r=1}^{m} \left\{ \int_l^e t_r \, \mathrm{d} \ln C_r + \int_e^i t_r \, \mathrm{d} \ln C_r + \int_i^h t_r \, \mathrm{d} \ln C_r \right\}, \tag{12}$$

where $\bar{t}_r$ and t_r denote the transfer numbers in the membrane and in the solution, respectively.

When $\bar{t}_r = t_r$, the right-hand side of eq. 12 corresponds to the liquid junction potential (ψ_L). When $\bar{t}_r \neq t_r$, we can write

$$\psi_M = \psi_L - \frac{RT}{F} \sum_{r=1}^{m} \int_l^i (\bar{t}_r - t_r)\, \mathrm{d} \ln C_r. \tag{13}$$

Integration of eq. 13 yields

$$\psi_M = \psi_L - \frac{RT}{F} \sum_{r=1}^{m} (\bar{t}_r - t_r) \ln\left[\frac{C_i}{C_e}\right]_r \tag{14}$$

where

$$\psi_S \equiv \frac{RT}{F} \sum_{r=1}^{m} (\bar{t}_r - t_r) \ln\left[\frac{C_i}{C_e}\right]_r \tag{15}$$

is the specific contribution [21].

Finally, comparison between eqs 15 and 10 for dilute solutions gives

$$(\mathrm{GEE})_k = \frac{RT}{F} \sum_{i=1}^{n} \sum_{r=1}^{m} (\bar{t}_r^i - t_r^i) \times \ln\left\{\left[\frac{C_i^i}{C_e^i}\right]_{r0} \left[\frac{C_i^i}{C_e^i}\right]_{rk}^{-1}\right\}. \tag{16}$$

For binary solutions and for a single-membrane system, eq. 16 transforms to the following form

$$(\mathrm{GEE})_k = \frac{RT}{F} (\Delta\bar{t} - \Delta t) \ln\left\{\left[\frac{C_i^i}{C_e^i}\right]_k \left[\frac{C_i^i}{C_e^i}\right]_0^{-1}\right\}, \tag{17}$$

where $\Delta\bar{t} = \bar{t}_- - \bar{t}_+$, $\Delta t = t_- - t_+$ and t is the electric transfer number of ions.

In order to express the ratio (C_i^i/C_e^i) in more suitable form for calculation, let us consider the membrane system depicted in fig. 2. We assume that this system contains the heterogeneous (not mechanically stirred) solutions of the same electrolyte at concentrations C_l and C_h, separated by an isotropic and symmetrical membrane. In this system, water and the dissolved substance diffusing across the membrane will lead to the formation of diffusion boundary layers on both sides of the membrane. These layers can be treated as membranes characterized by permeability coefficients ω_1^i and ω_2^i and by reflection coefficients σ_1^i and σ_2^i. The membrane has the corresponding reflection (σ_m) and permeability (ω_m) coefficients. The reflection and permeability coefficients of the boundary layer-membrane-boundary layer complex (b.l./M/b.l.) are denoted by σ_s^i and Ω_i. The solute flux across the boundary layer $(\mathrm{b.l.})_2$ is denoted by j_2^i, that across the membrane by j_m^i and that across the boundary layer $(\mathrm{b.l.})_1$ by j_1^i. The solute flux across the complex (b.l./M/b.l.) is represented by J_s^i. In the steady state, the following condition is satisfied

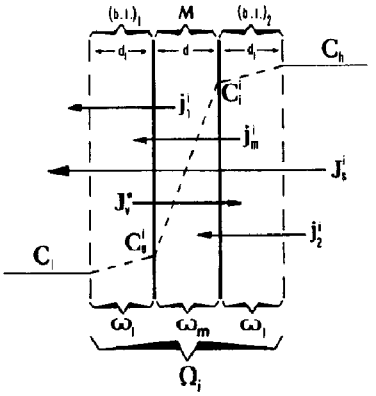

Fig. 2. The single-membrane system with the concentration profile. M, membrane; $(\mathrm{b.l.})_1$ and $(\mathrm{b.l.})_2$, boundary layers; C_l, C_e^i, C_i^i and C_h, solution concentrations; J_v^*, volume flux; j_1^i, j_2^i, j_m^i and j_s^i, solute fluxes; ω_1 and ω_m, permeability coefficients of boundary layers and membrane, respectively; Ω_i, permeability coefficient of the boundary layer-membrane-boundary layer complex; d_l and d, thickness of boundary layer and membrane, respectively.

$$j_1^i = j_m^i = j_2^i = J_s^i. \tag{18}$$

On the basis of the classical [27] and modified [23,24] forms of the second Kedem-Katchalsky equation, we can write

$$j_1^i = -\omega_1^i RT(C_e^i - C_l) + \bar{C}_1(1 - \sigma_1^i) J_v^i, \tag{19a}$$

$$j_m^i = -\omega_m RT(C_i^i - C_e^i) + \bar{C}_m(1 - \sigma_m) J_v^i, \tag{19b}$$

$$j_2^i = -\omega_2^i RT(C_h - C_i^i) + \bar{C}_2(1 - \sigma_2^i) J_v^i, \tag{19c}$$

$$J_s^i = -\Omega_i RT(C_h - C_l) + \bar{C}_s(1 - \sigma_s^i) J_v^i, \tag{19d}$$

where $\bar{C}_1 = \frac{1}{2}(C_e^i + C_l)$, $\bar{C}_2 = \frac{1}{2}(C_h + C_i^i)$, $\bar{C}_m = \frac{1}{2}(C_i^i + C_e^i)$, $\bar{C}_s = \frac{1}{2}(C_h + C_l)$ and J_v^i is the volume flux.

Combining eqs 18 and 19, assuming that $\sigma_1^i = \sigma_2^i = \sigma_i$ and $\omega_1^i = \omega_2^i = \omega_i$, we obtain

$$C_i^i = \xi\left\{C_h - \frac{\Omega_i}{\omega_i}(C_h - C_l) - \frac{J_v^i\{C_h[(1-\sigma_s^i)-(1-\sigma_i)] + C_l(1-\sigma_s^i)\}}{2\omega_i RT}\right\}, \quad (20)$$

$$C_e^i = \xi\left\{C_l + \frac{\Omega_i}{\omega_i}(C_h - C_l) - \frac{J_v^i\{C_l[(1-\sigma_s^i)-(1-\sigma_i)] + C_h(1-\sigma_s^i)\}}{2\omega_i RT}\right\}, \quad (21)$$

where $\xi = 2\omega_i RT[2\omega_i RT - (1-\sigma_i)J_v^i]^{-1}$.

On the basis of eqs 20 and 21 and using the expression [20]

$$\frac{1}{\Omega_i} = \frac{1}{\omega_m} + \frac{2}{\omega_i}, \quad (22)$$

the following equation is obtained

$$\begin{aligned}[C_i^i/C_e^i]_z &= (C_h/C_l)\big(1 + [C_l/C_h] \\ &\quad + (\Omega_i/\omega_m)(1 - [C_l/C_h] \\ &\quad - [(\omega_m - \Omega_i)J_v^i\{C_h(\sigma_m^i - \sigma_s^i) + C_l(1-\sigma_s^i)\}] \\ &\quad /[(2C_h\omega_m\Omega_i RT)]\big) \\ &\quad /\big(1 + [C_h/C_l] + (\Omega_i/\omega_m)(1 - [C_h/C_l] \\ &\quad - [\omega_m - \Omega_i])J_v^i\{C_l(\sigma_m^i - \sigma_s^i) + C_h(1-\sigma_s^i)\} \\ &\quad /[2C_l\omega_m\Omega_i RT]\big) \end{aligned} \quad (23)$$

where $z = 0, k$.

For $J_v^i = 0$, eq. 23 can be written in simpler form:

$$\left[\frac{C_i^i}{C_e^i}\right]_z = \frac{C_h}{C_l}\frac{\left(1 + \frac{C_l}{C_h}\right) + \frac{\Omega_i}{\omega_m}\left(1 - \frac{C_l}{C_h}\right)}{\left(1 + \frac{C_h}{C_l}\right) + \frac{\Omega_i}{\omega_m}\left(1 - \frac{C_h}{C_l}\right)}. \quad (24)$$

Regarding the expressions [25,27]

$$\frac{1}{\omega_i} = \frac{2RT}{D}\delta, \quad (25)$$

$$\delta = \left[\frac{R_c^* D_i \nu \rho_0}{g(\rho - \rho_0)}\right]^{1/3}, \quad (26)$$

on substitution into eq. 22, we obtain

$$\frac{\Omega_i}{\omega_m} = \frac{1}{1 + 2RT\omega_m\left[\frac{R_c^* \nu}{g\left(\frac{\rho}{\rho_0} - 1\right)D_i^2}\right]^{1/3}} \quad (27)$$

where R_c^* denotes the critical value of the concentration Rayleigh number, ν the kinematics viscosity, g the gravitational acceleration, ρ and ρ_0 the density of solution and solvent, respectively, and D_i the diffusion coefficient.

With the above being taken into consideration, eq. 17 together with eq. 23 or eqs 24 and 27 led to the model equation for the GEE being established. Below the experimental assessment of the validity of the model is described.

4. Experimental

4.1. Measuring system

Studies on the GEE in a single-membrane system were carried out by means of the experimental setup represented in fig. 3. The apparatus

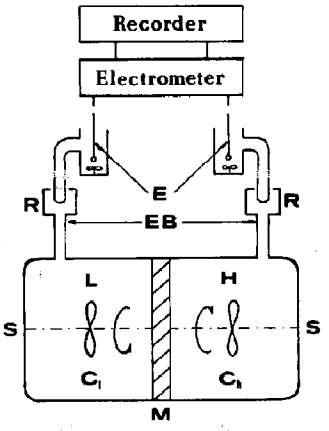

Fig. 3. Measuring system. M, membrane; C_l and C_h, solution concentrations; L and H, measuring vessels; s, stirrers; EB, electrolyte bridges; E, reversible electrodes; R, reservoirs of solutions.

Table 1

Membrane thickness and membrane permeability parameters for NaCl

Membrane	d (μm)	L_p ($\times 10^{12}$) (m^2/N per s)	σ ($\times 10^2$)	ω_m ($\times 10^{10}$) (mol/N per s)
Nephron [a]	200	5.0	6.0	14.3
Ultra-Flo 145 dialyzer [b]	800	0.85	16.7	5.5

[a] The properties of the Nephron membrane are similar to those of the Visking dialysis tubing used by Ginzburg and Katchalsky [27].
[b] Artificial Organs Division (Travenol Laboratories S.A., Brussels, Belgium).

consisted of a membrane system (UM), two outer Ag/AgCl electrodes (E) and elastic electrolytic bridges (EB). Details of the membrane system have been described elsewhere [22]. Compartment L of the membrane system in all experiments contained 0.001 M aqueous NaCl solution. Compartment H contained aqueous NaCl and/or ethanol at various concentrations. Both compartments were separated by one of the membranes listed in table 1. The vessels with the electrodes and the electrolytic bridges (EB) were filled with 1 M aqueous KCl-saturated AgCl. The Ag/AgCl electrodes were constructed according to the method of Ives [28]. All experiments were performed with vertically mounted electrodes. The membrane system and electrodes were placed in a thermostatted electrostatic shield. Measurements were taken at $T = (295 \pm 0.1)$ K.

5. Results

5.1. Effect of constraints release (ECR)

The ECR was examined for the three above-mentioned configurations of the membrane system (A, B_1 and B_2) according to the method in ref. 21. The same procedure was followed for each configuration. The first step involved measurement of the membrane potential (ψ_T), in the membrane system with mechanical stirring of the solution at 500 rpm. After achieving the initial steady state during which ψ_M was constant, stirring of the solutions was stopped, and subsequently the evolution of membrane potential was monitored up to the second steady state, when the transition potential (ψ_T) remains fixed. The data obtained thus are demonstrated in fig. 4. The evolution of the membrane potential (ψ_M) to the transition potentials ψ_{T0}, ψ_{T1} and ψ_{T2} is a reflection of the processes of formation of diffusion boundary layers on both sides of the membrane. Such behavior ceases on the attainment of a steady state. The ECR for all configurations was determined using eqs 3 and 4 on the basis of the measured values of ψ_M and ψ_T. The ECR is plotted as a function of (C_h/C_l) in fig. 5.

5.2. Transition potential (ψ_T) for binary solutions

From the experimental data depicted in fig. 4, it follows that the value of the membrane potential (ψ_M) does not depend on the configuration of

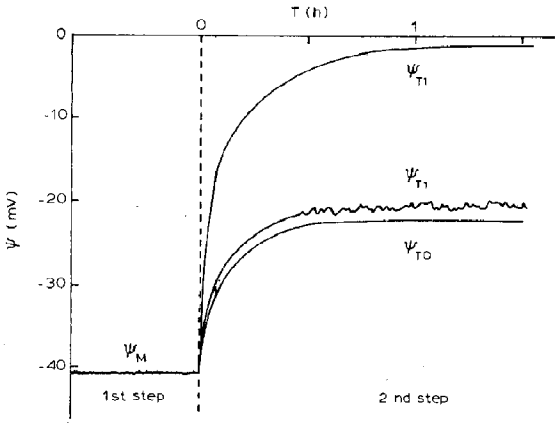

Fig. 4. Evolution of the membrane potential ψ_M in various configurations of the membrane system after turning off the mechanical stirrers. Transition potentials: ψ_{T0} (in configuration A); ψ_{T1} (configuration B_1) and ψ_{T2} (configuration B_2).

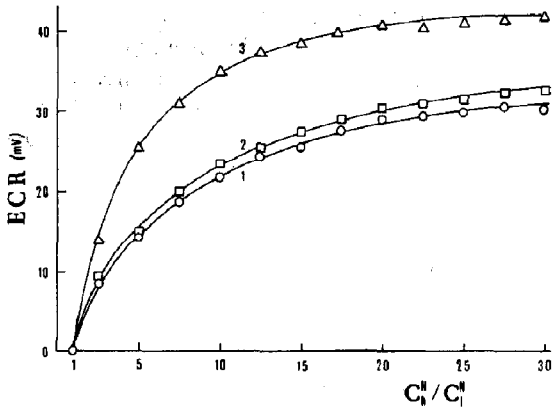

Fig. 5. Dependences ECR = $f(C_h^N/C_l^N)$. Curves: (1) configuration A, (2) configuration B_1, (3) configuration B_2.

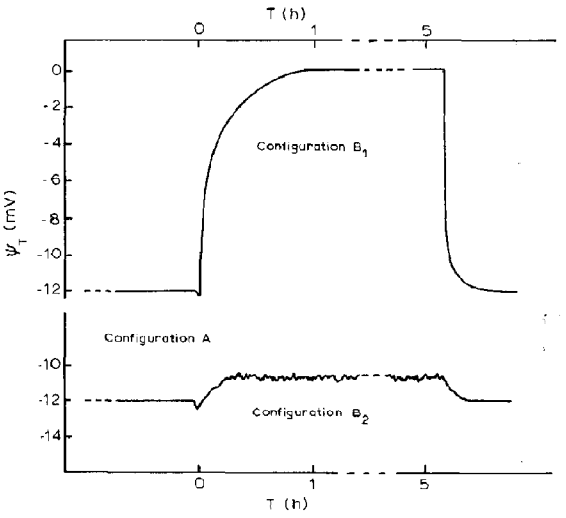

Fig. 6. Evolution of the transition potential (ψ_T) after reorientation of the membrane system from configuration A to B_1 and from A to B_2.

the membrane system. This signifies that $\psi_M - \psi_{Mk} = 0$. As a consequence

$$(GEE)_k = (\psi_T)_k - (\psi_T)_0. \quad (28)$$

In order to study the GEE and to assess the validity of eq. 28, the membrane system in which the solutions were not mechanically stirred was used. One experiment involved orienting the membrane system in configuration A. After attaining a steady state in which ψ_T = constant, the orientation was altered by rotation through 90° to result in configuration B_1. In another experiment, the same procedure was carried out, to give rise to configuration B_2. Fig. 6 illustrates the procedure. From the curves depicted in fig. 6, it is evident that a change in configuration from A to B_1 or B_2 leads to a change in transition potential from ψ_{T0} to ψ_{T1} or ψ_{T2}. Additionally, one observes that reorientation of the membrane system from configuration A to B_1 results in a substantially greater extent of the GEE as compared to that from A to B_2. In the former case, the complex of the diffusion boundary layer is hydrodynamically stable whereas it displays instability in the latter, as confirmed by the function ψ_{T2} in the steady state.

5.3. Concentration dependence of the GEE for binary and ternary solutions

The results obtained for the GEE are presented in figs 7 and 8. The data illustrating the depen-

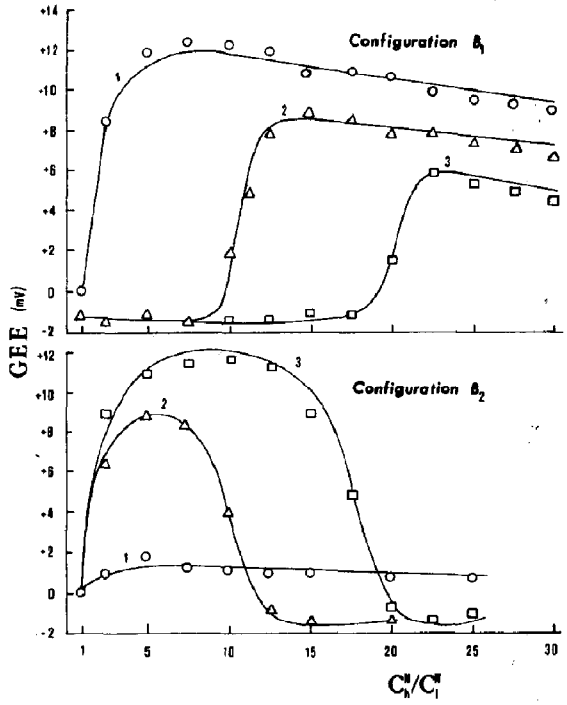

Fig. 7. Experimental and calculated GEE as a function of (C_h^N/C_l^N) in binary (1) and in ternary solutions (2 and 3): (○) no ethanol; (△) $C_n^E = 0.05$ M; (□) $C_n^E = 0.1$ M. (———) GEE calculated on the basis of eqs 17 and 24 after taking into consideration $\Omega_i(C)$.

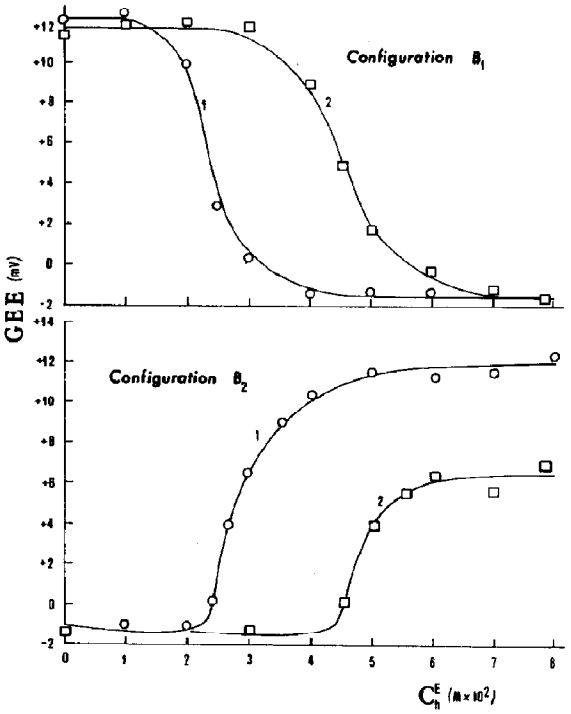

Fig. 8. Experimental and calculated GEE as a function of ethanol concentration (C_h^E): $C_h^N C_l^N = 5$ (○), $C_h^N C_l^N = 10$ (□). (———) GEE calculated on the basis of eqs 17 and 24 after taking into consideration $\Omega_i(C)$. Curves 1 and 2 were obtained for ternary solutions.

dence GEE $= f(C_h^N/C_l^N)$ are shown in fig. 7 for solutions of fixed ethanol concentration and varying NaCl concentration (C_h^N). For binary solutions progressive addition of NaCl increases the density of solutions. For the solutions containing 0.05 and 0.1 M ethanol, progressive NaCl addition increases the density from below to above that of a 0.001 M aqueous NaCl solution. Fig. 8 displays the data recorded at constant NaCl concentration and varying ethanol levels. In contrast to the preceding case, progressive addition of ethanol to 0.005 and 0.01 M NaCl lowers the density from above to below that of a 0.001 M aqueous solution of NaCl.

The arrows in figs 7 and 8 indicate those ternary compositions for which the density matches that of a 0.001 M aqueous solution of NaCl. Significantly, the most extensive changes in GEE occur at these compositions. In ref. 25, the type of change in J_v^* and J_s^* was discussed in relation to the gravitational instability or stability of the boundary layers, i.e., low experimental values of J_v^* or J_s^* indicate that the boundary layers are stable whereas high values correspond to their being unstable. Analogously, we interpret a low observed GEE as reflecting the instability of boundary layers in configurations A and B, whilst high values are indicative of their stability in configuration B_1.

5.4. Experimental verification of the GEE model equation being valid for a single-membrane system

In order to establish the validity of the GEE model equation, the parameters Ω_i, ω_m, ν, ρ and $\Delta\bar{t}$ for NaCl and/or ethanol were evaluated experimentally. The values of $\Delta\bar{t}$, determined according to the method of Laksminarayanaiah [20] at various concentrations of NaCl solution and using different membranes, are plotted in fig. 9. The values of Δt in solution were determined using the reported values for t_- and t_+ [29] ($t_- = 0.608$, $t_+ = 392$). Since the magnitude of such transfer numbers is practically independent of solution concentration, then $\Delta t = 0.216$. The values of the parameters Ω_i and ω_m were determined by the standard isotope method, details of which are given in ref. 30. The values of the above parameters for NaCl and ethanol are listed in tables 1 and 2, those of ρ and ν being collected in tables 3 and 4.

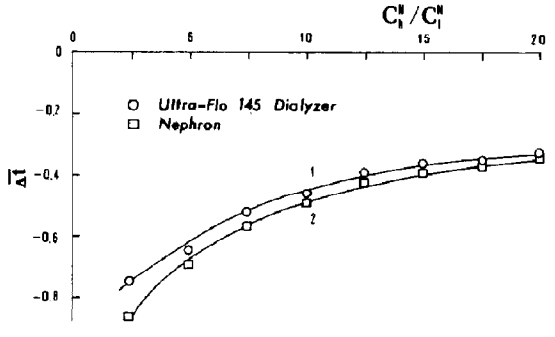

Fig. 9. Dependences $\Delta\bar{t} = f(C_h^N/C_l^N)$ for membrane: Ultra-Flo 145 Dialyzer (1) and Nephron (2).

Table 2

Values of coefficients Ω_i and σ_{si} for NaCl

Membrane	Configuration	Ω_i ($\times 10^{10}$) (mol/N per s)	σ_{si} ($\times 10^2$)
Nephron	vertical A	5.2	2.0
	horizontal B_1	0.7	0.14
	horizontal B_2	5.4	1.9
Ultra-Flo 145 dialyzer	vertical A	2.65	5.1
	horizontal B_1	0.45	0.7
	horizontal B_2	2.85	5.0

Eqs 17 and 24 are applicable for the analysis of the GEE in single-membrane system. Consider the results shown in figs 7 and 8. It is clearly evident from these figures that the behavior of GEE = $f(C)$ is nonlinear. In the case of binary solutions, one can use eqs 17 and 24 to describe the GEE with the values of ω_m and Ω_i being assumed, as listed in tables 1 and 2. However, for ternary solutions, one also requires knowledge of the dependence of Ω_i upon the concentration and configuration of the system in order to carry out the aforementioned analysis. That such an assumption is indeed valid is borne out by the data depicted in figs 10 and 11.

Curves 1 and 2 in fig. 10 represent the dependence on NaCl concentration for the experimentally determined factor Ω_N/ω_N (at constant ethanol content) for configuration B_1. This factor,

Table 3

Values of the density (ρ) and kinematic viscosity (ν) of ternary water-sodium chloride-ethanol solutions for various concentrations of sodium chloride (C_h^N) and constant ethanol content (C_h^E)

C_h^N (mol/l)	ρ ($\times 10^{-3}$) (kg/m^3) at C_h^E:			ν ($\times 10^6$) (m^2/s) at C_h^E:		
	0 M	0.05 M	0.1 M	0 M	0.05 M	0.1 M
0.001	0.99739	0.99707	0.99675	0.9977	1.0079	1.0183
0.0025	0.99733	0.99711	0.99679	0.9977	1.0079	1.0183
0.005	0.99741	0.99719	0.99686	0.9976	1.0078	1.0182
0.0075	0.99749	0.99726	0.99704	0.9975	1.0078	1.0180
0.01	0.99756	0.99734	0.99712	0.9974	1.0077	1.0179
0.0125	0.99764	0.99741	0.99720	0.9973	1.0076	1.0178
0.015	0.99771	0.99749	0.99727	0.9973	1.0075	1.0178
0.0175	0.99779	0.99757	0.99735	0.9972	1.0074	1.0177
0.02	0.99787	0.00764	0.99742	0.9971	1.0074	1.0176
0.0225	0.99795	0.99771	0.99749	0.9970	1.0073	1.0175
0.025	0.99802	0.99779	0.99757	0.9970	1.0072	1.0174

Table 4

Values of the density (ρ) and kinematic viscosity (ν) of ternary water-sodium chloride-ethanol solutions for various concentrations of ethanol (C_h^E) and constant sodium chloride content (C_h^N)

C_h^E (mol/l)	ρ ($\times 10^{-3}$) (kg/m^3) at C_h^N:			ν ($\times 10^6$) (m^2/s) at C_h^N:		
	0.001 M	0.005 M	0.01 M	0.001 M	0.005 M	0.01 M
0.01	0.99716	0.00738	0.99759	0.99984	0.99962	0.99940
0.015	0.99713	0.99734	0.99755	1.00087	1.00066	1.00045
0.02	0.99709	0.99730	0.99750	1.00190	1.00150	1.00151
0.025	0.99704	0.99726	0.99748	1.00300	1.00270	1.00250
0.03	0.99700	0.99722	0.99743	1.00400	1.00380	1.00360
0.04	0.99692	0.99713	0.99734	1.00610	1.00590	1.00570
0.05	0.99684	0.99705	0.99727	1.00820	1.00800	1.00770
0.06	0.99670	0.99698	0.99719	1.01030	1.01000	1.00980
0.07	0.99667	0.99698	0.99711	1.01240	1.01210	1.01200
0.1	0.99643	0.99665	0.99687	1.01860	1.01840	1.01820

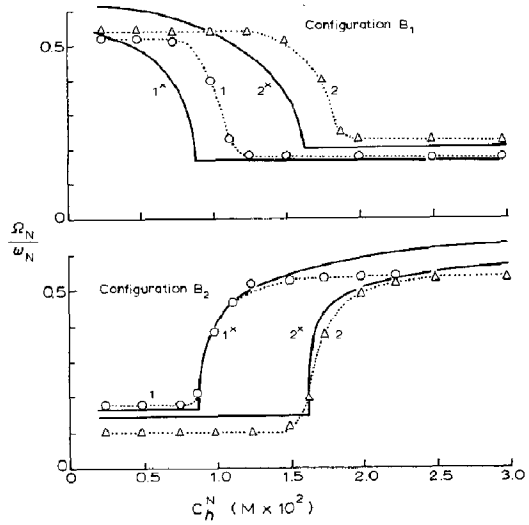

Fig. 10. Concentration dependence of the factor Ω_N/ω_N determined experimentally (curves 1 and 2) and calculated on the basis of eq. 27 (curves 1* and 2*) for NaCl in aqueous ethanol solution of 0.05 M (1 and 1*) and 0.1 M (2 and 2*).

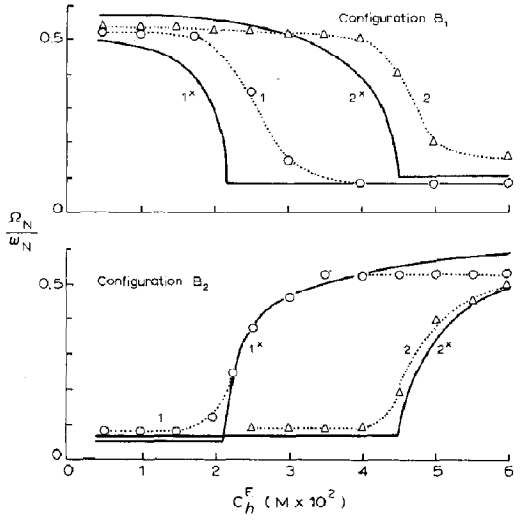

Fig. 11. Concentration dependence of the factor Ω_E/ω_E determined experimentally (curves 1 and 2) and calculated on the basis of eq. 27 (curves 1* and 2*) for 0.005 M NaCl (1 and 1*) and 0.01 M NaCl (2 and 2*) in various aqueous ethanol solutions.

furthermore, depends on the ethanol concentration, as illustrated by curves 1 and 2 in fig. 11. Curves 1* and 2* in figs 10 and 11 were obtained via calculation of Ω_N/ω_N on the basis of eq. 27. For the calculation, the following published values were taken: $R_c^* = 150$ [31] and $D = 1.57 \times 10^{-9}$ m^2/s [32].

As demonstrated by the data in figs 10 and 11, for B_1 the experimental and calculated values of Ω_N/ω_N diverge whereas for B_2 they show good agreement (eq. 27 being used for the evaluation of the above factor). The results are comparable with those obtained for volume flux in the previous article [25]. The variation in the GEE was calculated, based on eqs 17 and 24, as a function of C_h^N/C_l^N or C_h^E, with the experimental Ω_N/ω_N concentration-dependent behavior in figs 10 and 11 and parameter values listed in table 2 being taken into account. The unbroken lines in figs 7 and 8 correspond to the data obtained via calculation of the GEE. The results obtained experimentally and those from calculation are consistent with each other and, hence, eqs 17 and 24 yield a satisfactory fit to the curves from experiment, when the concentration dependence of $\Omega(C)/\omega$ is taken into consideration.

6. Conclusions

It has been demonstrated herein that the model equation for the GEE may be employed in interpreting the data recorded on the gravielectric polarization in a single-membrane system. However, this is possible only when the dependence of Ω/ω on concentration is known. The values of these parameters are governed by the hydrodynamic state of the boundary layer-membrane-boundary layer complex. The expression for this factor should contain the Rayleigh number, solution density and kinematic viscosity, and gravitational acceleration, etc. The initial point of convection is determined by the critical Rayleigh number. On relation to the GEE in a single-membrane system, one can assess whether natural convection will appear in a two-membrane system.

References

1 A.A. Gordon and M.J. Cohen, Gravity and the organism (University of Chicago Press, Chicago, 1971).
2 S.J. Gould, Evolution 21 (1966) 385.
3 A.J. Hodspeth, Science 230 (1985) 745.
4 J. Neubert, W. Briegleb and A. Schatz, Naturwissenschaften 73 (1986) 428.
5 L.J. Audus, J. Exp. Bot. 30 (1979) 1051.
6 B. Bean, in: Membranes and sensory transduction, eds G. Colombetti and F. Lenci (Plenum, New York, 1984) p. 163.
7 R. Moore and M.L. Evans, Am. J. Bot. 73 (1986) 574.
8 J. Bose, Comparative electrophysiology (Longmans Green, London, 1907).
9 L. Brauner, Kolloidchem. Beih. 23 (1926) 143.
10 L. Brauner, Planta 53 (1959) 449.
11 L. Brauner, Endeavour 28 (1970) 17.
12 L. Grahm and C.H. Hertz, Physiol. Plant. 17 (1964) 187.
13 A.C.R. Woodcock and M.B. Wilkins, J. Exp. Bot. 20 (1969) 156; J. Exp. Bot. 22 (1971) 512.
14 B. Etherton and R.R. Dedolph, Plant. Physiol. 49 (1972) 1019.
15 H.M. Beherens, A.D. Gradman and A. Sievers, Planta 163 (1985) 463.
16 H.C. Custard and C.R. Faris, Planta 65 (1965) 83.
17 P.H. Barry and J.M. Diamond, Physiol. Rev. 64 (1984) 763.
18 K. Inenaga and N. Yoshida, J. Membrane Sci. 6 (1980) 271.
19 A. Ślęzak and K. Dworecki, Stud. Biophys. 100 (1984) 41.
20 N. Lakshiminarayanaiah, Transport phenomena in membranes (Academic Press, New York, 1969).
21 A. Rejou-Michel, A. Villardi and M. Delmotte, Bioelectrochem. Bioenerg. 6 (1979) 189.
22 A. Ślęzak, Biophys. Chem. 34 (1989) 91.
23 A. Ślęzak and B. Turczyński, Biophys. Chem. 24 (1986) 173.
24 A. Ślęzak, B. Turczyński and Z. Nawrat, J. Non-Equilib. Thermodyn. 14 (1989) 205.
25 A. Ślęzak, K. Dworecki and J.E. Anderson, J. Membrane Sci. 23 (1985) 71.
26 A. Ślęzak, J. Membrane Sci. 26 (1986) 115.
27 A. Katchalsky and P.F. Curran, Nonequilibrium thermodynamics in biophysics (Harvard University Press, Cambridge, 1965).
28 S.G.J. Ives and G.J. Janz, Reference electrodes (Academic Press, New York, 1961).
29 B.E. Convay, Theory and principles of electrode processes (Roland Press, New York, 1965).
30 H.H. Ussing, in: Membrane transport in biology, eds G. Giebisch, D.C. Tosteson and H.H. Ussing (Springer, Berlin, 1978) p. 115.
31 A. Ślęzak, Postępy Fiz. Med. 25 (1990) in the press.
32 R.A. Robinson and R.H. Stokes, Electrolyte solutions (Butterworths, London, 1959).